PROJECT 1.2: SOUTH-WEST WESTERN AUSTRALIA'S REGIONAL SURFACE CLIMATE AND WEATHER SYSTEMS

Principal Investigator

Pandora Hope, Bureau of Meteorology, Centre for Australian Weather and Climate Research, PO Box 1289, Melbourne, Victoria, 3001 (Ph: 03 9669 4774; Email: p.hope@bom.gov.au);

Senior Investigators

Kevin Keay, Bureau of Meteorology, Centre for Australian Weather and Climate Research, PO Box 1289, Melbourne, Victoria, 3001 (Ph: 03 9616 8341; Email: k.keay@bom.gov.au)

Catherine J Ganter, Bureau of Meteorology, National Climate Centre, PO Box 1289, Melbourne, Victoria, 3001 (Ph: 03 9669 4679; Email: c.ganter@bom.gov.au)

Collaborators (not funded by IOCI)

Pauline Treble, Australian Nuclear Science and Technology Organisation, Institute for Environmental Research, Locked Bag 2001 Kirrawee DC NSW 2232 (Ph: 02 9717 9356) Email: ptr@ansto.gov.au

Alan Wain, Bureau of Meteorology, Centre for Australian Weather and Climate Research, PO Box 1289, Melbourne, Victoria, 3001 (Ph: 03 9669 4711) Email: a.wain@bom.gov.au

Objectives of Project 1.2

- To determine if seasonal rainfall across the wider South-West is showing new trends in totals or shifts in intensity.
- To determine whether there has been a shift to a new weather regime in recent years.
- To determine whether observed changes are likely to continue into the future.

- To place the current multi-decade rainfall decline in the context of the last few 100 years.

Planned Outcomes of this Milestone Report

To determine if the synoptic types described in previous Milestone reports for each season display changes into the future under two different future scenarios.

Describe the potential and limitations for developing a reliable reconstruction of the past hydro-climate of SWWA from speleothem isotopes.

Key Research Findings

1. There was a particular synoptic type prevalent during the low puerulus return year of 2008 in the new half-year SOM. It had off-shore winds associated with it, and occurred most commonly in July and August. This type will increase in frequency under future scenarios.
2. All seasons show fewer occurrences of synoptic types displaying regions of low pressure through the domain and more occurrences of those with high pressure under both future scenarios at the end of this century compared to the end of the last century.
3. The summer changes were emphatic even at mid-century. The temperature anomalies associated with these changes suggest warmer than average conditions along the west coast but that the eastern extent of SWWA might have its summer maximum temperatures ameliorated by the prevailing circulation conditions.
4. Cave stalagmites are well located in the south-west to provide a proxy record of rainfall through the last few hundred years at least. There are no other proxies currently available in the vicinity. The isotopic values expressed in cave stalagmites in general correspond well with rainfall variability; however, shifts in the circulation can confound this relationship.
5. An understanding of the variability of the dominant circulation and rainfall through the last few hundred years may be gained by combining proxy measures and knowledge of the circulation that impacts SWWA and its regional effects. Records of precipitation from Antarctica that have been

linked to rainfall in SWWA show anomalies over the past few decades outside the range of variability of the last 750 years.

Milestone 1.2.3 *Report on the range of weather systems identified by the new classification scheme for South-West summer weather systems*

(Completed 31/12/2010)

This milestone was reported on extensively in IOCI3 milestone report 2 and finalised in milestone report 3.

Milestone 1.2.4 *Report on the range of weather systems identified by the new classification scheme for South-West spring and autumn weather systems***.** (**Completed 31/12/2010**)

This milestone was reported on extensively in IOCI3 milestone report 3.

Milestone 1.2.5 *Report on the time series of these systems in the observations*

(Report extending previous progress reports is below.)

June & July

The time-series of these synoptic types from NCEP/NCAR reanalyses (NNR; Kalnay et al. 1996) were discussed extensively in Hope et al., 2006. Results from recent years were also discussed in IOCI3 Milestone report 1. The time-series of types associated with deep low pressure systems and those associated with an extensive high across the region have been used in a number of presentations to IOCI partners and others, and that slide is shown here for information.

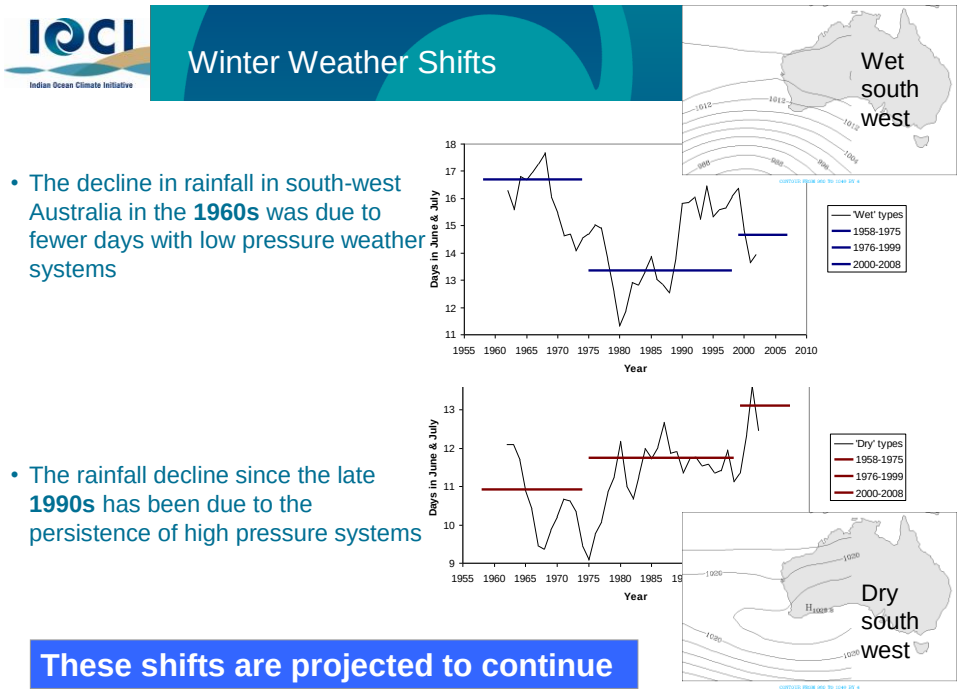

Figure 1. Slide showing the limited change in the number of deep low pressure systems (wet across the south-west) compared to the strong increase in the number of strong high pressure systems (dry across the region), and how this change differs from the changes seen in the 1970s.

Spring (extended)

The time-series of this range of synoptic systems were discussed in the previous milestone report. After discussion with Nick Caputi from WA Fisheries, this IOCI work was extended to align better with their analysis. Thus further reporting will now be based on a new SOM developed in collaboration with them (Figure 2). It includes the months from July to December.

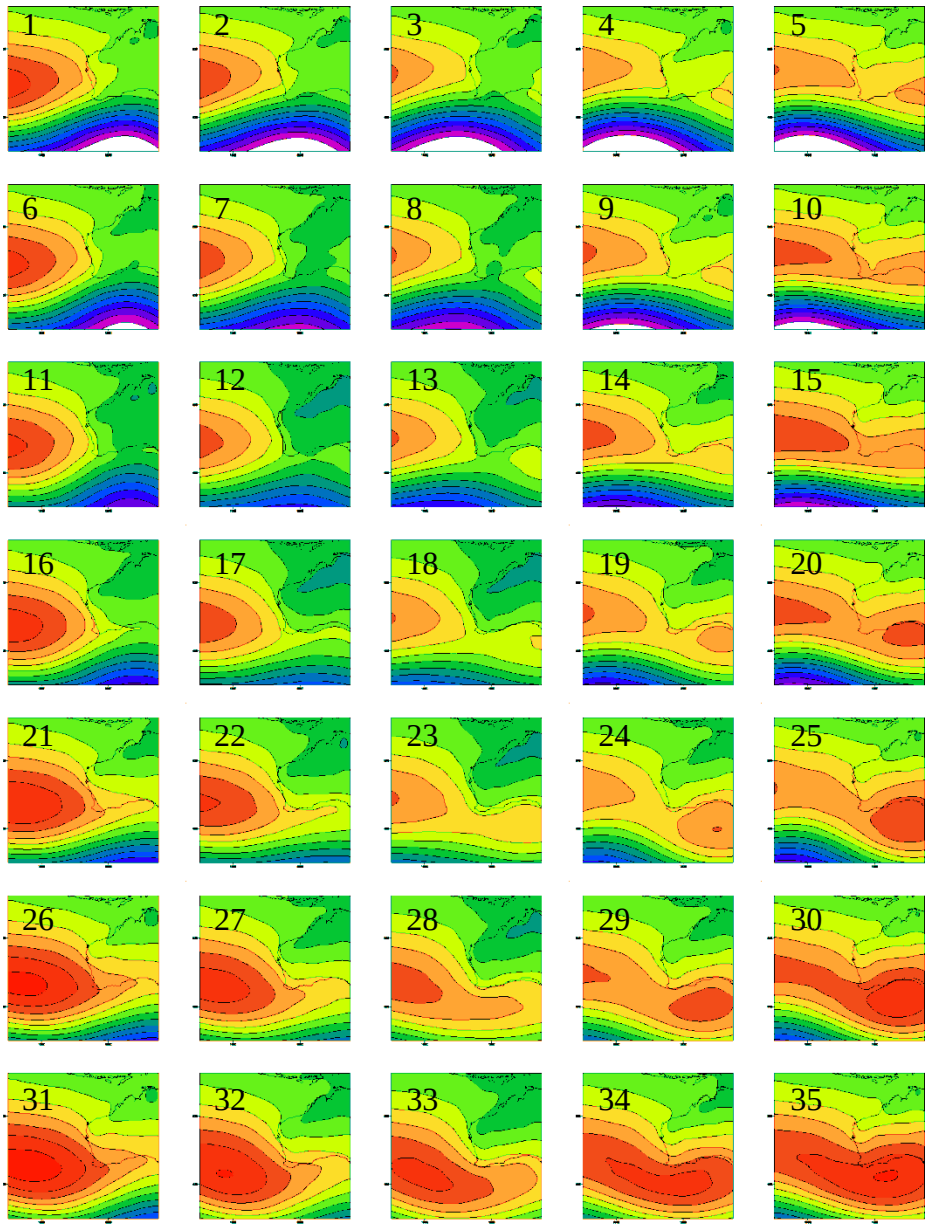

Figure 2. SOM for MSLP 1948-2010 JASOND 2pm (06UTC).

As noted in previous IOCI3 milestone reports, there was a particular synoptic type, with off-shore winds, that was prevalent in the year of low puerulus settlement in 2008. This is still the case, as type 35 is dominant during 2008 (Figure 3), and has off-shore winds (Figure 4).

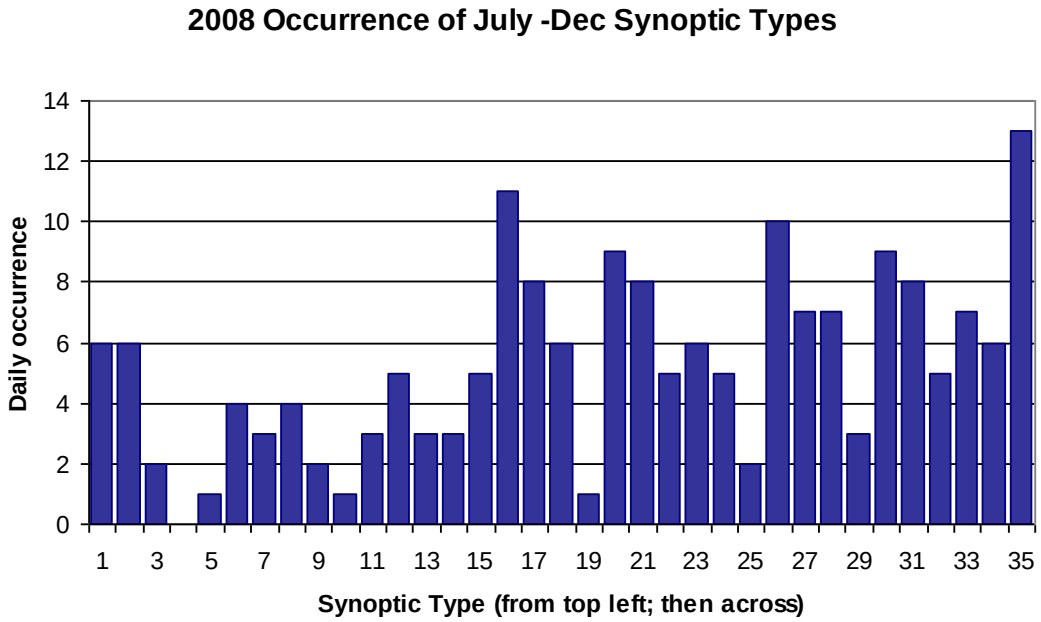

Figure 3. The daily occurrence of each synoptic type in the July-December SOM in 2008. Type 35 (bottom right of the SOM in Figure 2) was most prevalent

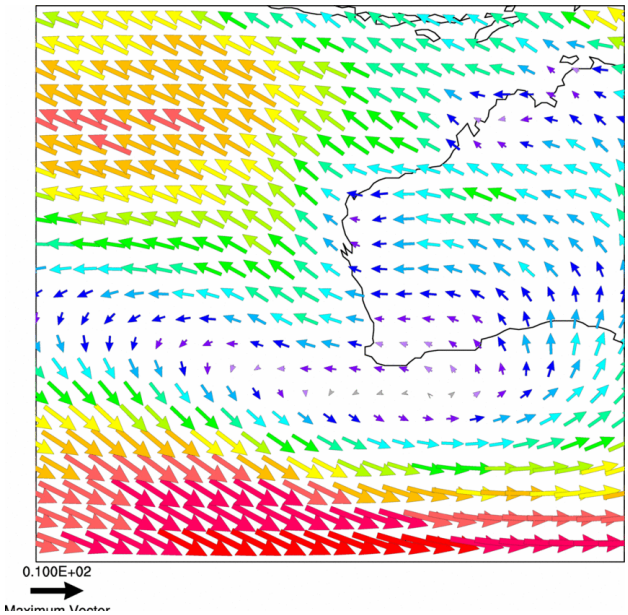

Figure 4: Arrows indicate wind direction and strength (larger red arrows = stronger winds). This figure shows the composite winds for synoptic type 35 from the SOM.

However, the association is not simple, given that this SOM covers half the year, the timing of the various synoptic types may also be important to the rock-lobster life-cycle. To this end, the monthly distribution within each synoptic type during 2008 was explored (Figure 5). It was found that the large contribution from the

off-shore winds of type 35 occurred predominantly in August. Type 35 is also becoming more common - 0.68 more occurrences per year from 1968 to 2010.

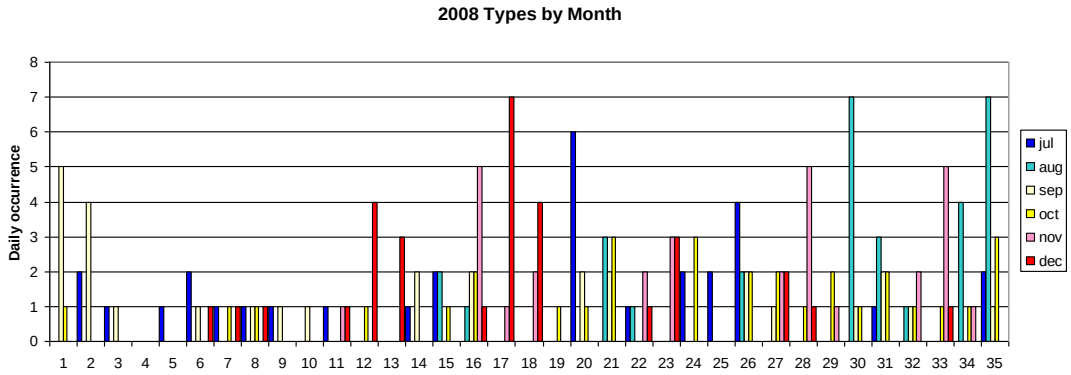

Figure 5. The month within which each occurrence of each synoptic type occurs in 2008.

There are clearly other factors that influence puerulus settlement aside from the synoptic situation, however, this is one factor that we can consider into the future under a range of emission scenarios. Thus, once we understand how these different factors contribute to the life-cycle of the rock-lobster, we'll be able to say a little more about what the future holds for the industry.

Summer

The timeseries of the summer synoptic types were considered in the previous milestone report under Milestone 1.2.3. The trends of the important synoptic types, linked to cooler maximum temperatures, will be assessed for their representation in climate models both under present conditions and for future scenarios (Milestones 1.2.6 and 1.2.7 respectively).

Autumn

This was completed in the previous milestone report under Milestone 1.2.5.

Milestone 1.2.6 *Report on whether these systems are expressed in climate model simulations*

The self-organising map was chosen as the method for assessing the weather types that impact SWWA across all seasons and research questions. Thus, the method employed by Hope (2006) was used for identification of these types in climate model output.

Due to a range of issues, World Climate Research Programme's (WCRP's) Coupled Model Intercomparison Project phase 3 (CMIP3) multi-model dataset (Meehl et al., 2007) has been used rather than the more recent CMIP5 (described in Taylor et al., 2012). This is due to a delay in the transfer of results from the individual modelling institutions, and data transfer and storage limitations. We acknowledge the modeling groups, the Program for Climate Model Diagnosis and Intercomparison (PCMDI) and the WCRP's Working Group on Coupled Modelling (WGCM) for their roles in making available the WCRP CMIP3 multi-model dataset. Support of this dataset is provided by the Office of Science, U.S. Department of Energy. Only one realisation from each model was used.

Table 1. Daily data were obtained from the modelling groups listed below via PCMDI. Note that not all groups have a letter against them. This is because, although model results from BCC-CM1 and INM-CM3.0 were analysed, their data appeared to have major concerns. It is not clear at what stage those errors appeared in the data, but it was un-usable. *The archive of the 20th century ensemble member of CSIRO-Mk3.0 used by Hope (2006) has been corrupted since 2006, so a second member was used.

No	Originating Group(s)	Country	CMIP3 I.D.
	Beijing Climate Center	China	BCC-CM1
a	Canadian Centre for Climate Modelling & Analysis	Canada	CGCM3.1(T47)
	Canadian Centre for Climate Modelling & Analysis	Canada	CGCM3.1(T63)

b	Météo-France / Centre National de Recherches Météorologiques	France	CNRM-CM3
c	CSIRO Atmospheric Research	Australia	CSIRO-Mk3.0*
d	CSIRO Atmospheric Research	Australia	CSIRO-Mk3.5
e	US Dept. of Commerce / NOAA / Geophysical Fluid Dynamics Laboratory	USA	GFDL-CM2.0
f	US Dept. of Commerce / NOAA / Geophysical Fluid Dynamics Laboratory	USA	GFDL-CM2.1
g	NASA / Goddard Institute for Space Studies	USA	GISS-ER
	Institute for Numerical Mathematics	Russia	INM-CM3.0
h	Institut Pierre Simon Laplace	France	IPSL-CM4
i	Center for Climate System Research (The University of Tokyo), National Institute for Environmental Studies, and Frontier Research Center for Global Change (JAMSTEC)	Japan	MIROC3.2(medres)
j	Meteorological Institute of the University of Bonn, Meteorological Research Institute of KMA, and Model and Data group.	Germany / Korea	ECHO-G
k	Max Planck Institute for Meteorology	Germany	ECHAM5/MPI-OM
l	Meteorological Research Institute	Japan	MRI-CGCM2.3.2
m	National Center for Atmospheric	USA	PCM

The range of synoptic types as represented by NCEP/NCAR reanalyses (NNR) was shown for each season (and research question) with a self-organising map (SOM) in earlier milestones. The method encourages the development of synoptic types that capture the continuum of the daily data considered and a reasonably even distribution across the types. As each SOM has a different number of days within it, we show the number of days per season that fall into each type. This differs with each season's SOM, and thus the scales vary, but for an even distribution across all the synoptic types, colours should be close to the dark green/bright green divide in the plots below. The expected number of days per season for each season's SOM is shown in Table 2.

Table 2

Months in Season	Mean Days per type per season	Equation
June, July	3.05	61 days/((4*5) types)
July,A,S,O,N,Dec	5.26	184/(5*7)
January, February	4.92	59/(3*4)
March, April, May	4.60	92/(4*5)

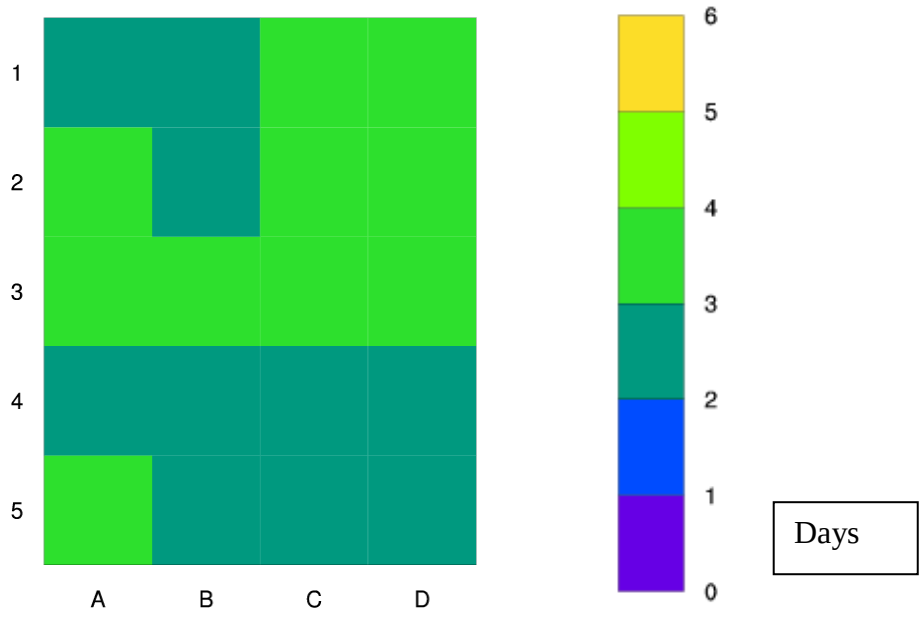

Figure 6 - JJ_NNR. Counts of each synoptic type in NNR for the June and July SOM. The expected count in each type given an even distribution is approximately 3.

Figure 6 shows that the occurrence of each type (standardised to a scale of days/season) in the June and July SOM. An even distribution would be of the order of 61/20 ≈ 3 in each type, and we see that each type has approximately 3 days per season in it.

To determine whether the models can represent this range of types, the count per season was calculated for each climate model (see Appendix, Figure A1). One of the types within the SOM, D5, is not well represented by five of the 13 models. Type D5 has a deep low to the south and west of SWWA. Four of the five models that do not capture this type well have higher pressures in their mean MSLP to the south-west of the region compared to the other models. Model b, CNRM-CM3, also shows fewer of the more extreme types, and a higher occurrence of a type closer to the mean. Even with these inter-model differences, all types are still represented by all models. Thus, it is clear that the models can and do capture the range of synoptic types that have been identified using NNR for the June and July case.

The SOM representing the synoptic types from July to December covers a wide range of types. The NNR distribution across the types is reasonably even (Figure

7). In some cases some synoptic types have a low representation by some models (Appendix, Figure A2), however there is no consistency in a low representation of any one type across the models, and no models completely miss any types.

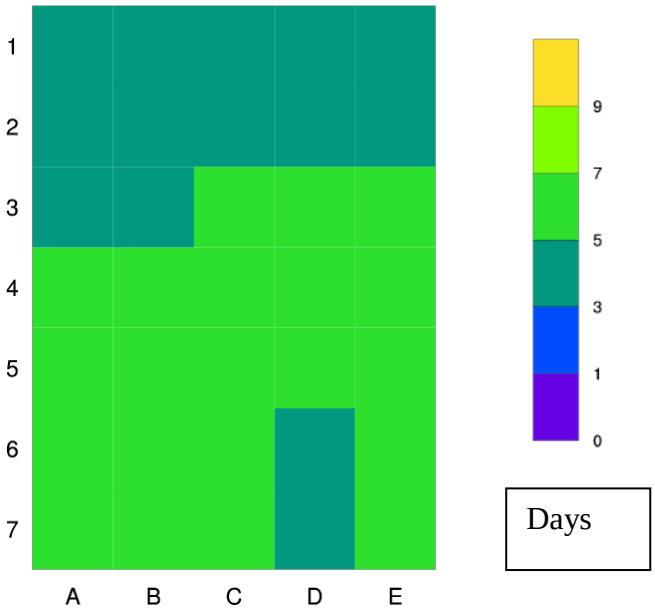

Figure 7 - JASOND_NNR. Counts of each synoptic type in NNR for the July to December SOM. The expected count in each type given an even distribution is 5.3

The January and February SOM represents a range of 12 synoptic types and all models capture all these types (see Appendix Figure A3).

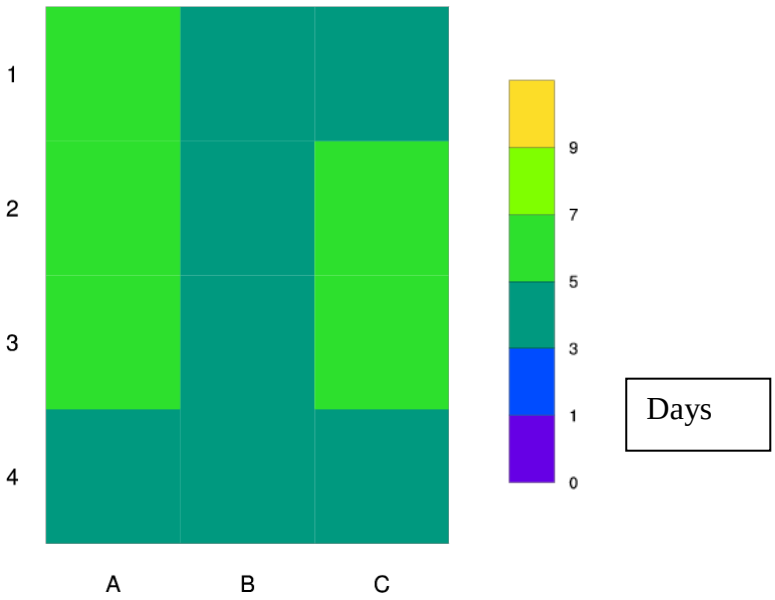

Figure 8 - JF_NNR. Counts of each synoptic type in NNR for the January and February SOM. The expected count in each type given an even distribution is 4.9

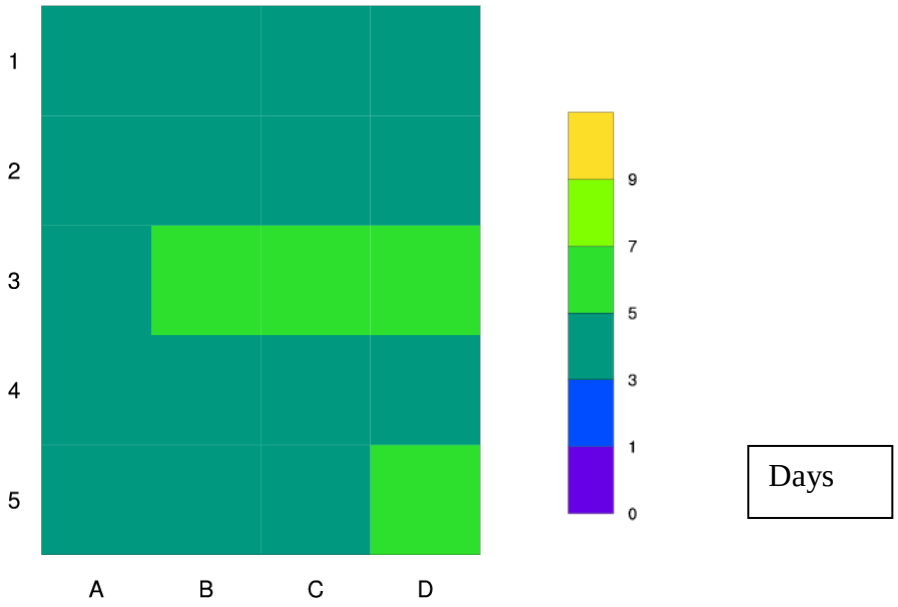

Figure 9 - MAM_NNR. Counts of each synoptic type in NNR for the March to May (autumn) SOM. The expected count in each type given an even distribution is 4.60.

The MAM SOM types are evenly distributed across the SOM for NNR (Figure 9). For most models this is also the case (see Appendix Figure A4). However, Model b has a stronger signal from the 'mean' state (more central nodes of the SOM) rather than the types with more 'extreme' features across the region.

For all SOMs, the models of the late 20th century can all capture the synoptic types represented by the NNR. In general, with only a few exceptions, this distribution is reasonably even.

Milestone 1.2.7 *Report on whether these systems change in frequency in simulations of future scenarios*

Daily climate model data from 15 different models (outlined in milestone above) were used to determine how the frequency of the synoptic types in each season's SOM change under two different future emissions scenarios and for the periods 2046-2065 and 2081-2100. These periods were chosen primarily because daily data were available. The two emission scenarios were SRES A2, a high emissions scenario ('business as usual') which we are tracking at or above in reality; the second was SRES B1, a low emissions scenario which would require significant

reduction of current emissions. Using the two scenarios allows an appreciation of the impact of a strengthening greenhouse gas signal. Through time the level of greenhouse gases increases in both scenarios through to the end of the century.

The mean of the models was calculated using a number of steps. First, the mean daily occurrence of each synoptic type for the future period and the present-day (1961-2000) period were calculated. Then the percentage change between these was calculated for each model.

percentage change =
*(mean number of events per season in future) - (mean number of events per season in 20th century) / (mean number of events per season in 20th century) * 100*

The mean of these changes was then calculated and the significance of the mean change was calculated using a number of methods.

As a first test, the significance of the change from the 20th to the 21st century for each synoptic type and each individual model was calculated using an unpaired t-test. Plots showing the percentage change for each model, with an '*' indicating significance of this change at the 5% level are shown in the Appendix (Figure 10). It is clear that almost all the models show the same signature of change as expressed by the multi-model mean (Figure 11). In all other seasons and cases, only the multi-model mean will be shown, with a range of tests on the significance of the changes.

The first method tests for consensus among the models on their direction of change (Power et al., 2011). The method is based on a binomial distribution with sample size M (the number of models) and the probability of occurrence of either sign (positive or negative) p = 0.5 i.e. either sign is equally likely. For the 13 models of SRESA2 we require ≥ 10 occurrences of the same sign; for the 12 models of SRESB1 it is ≥ 9 (Figure 10). A '+' indicates significance of consensus at the 5% level, and this test is overlaid on the multi-model mean percentage change plots in the left-hand column of Figures 11, 7, 8, 9.

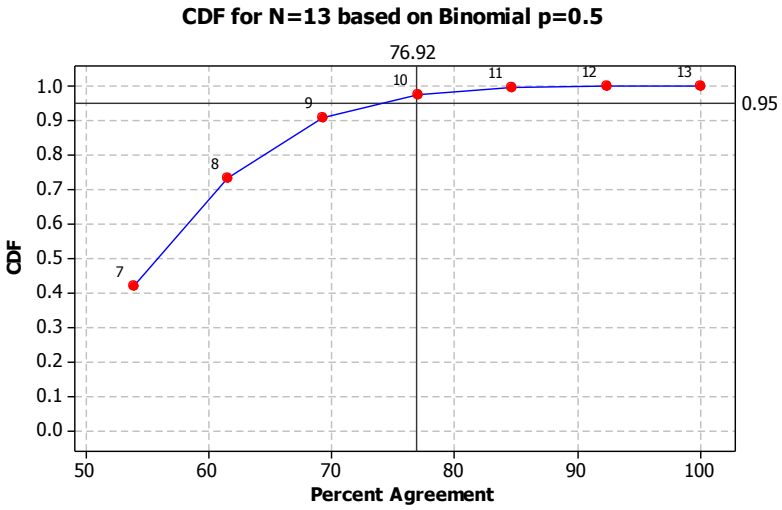

Figure 10- test. Plot showing the probability distribution of the binomial distribution of the ensemble of percentage change for 13 models. The 95% level of significance is shown and indicates that 10 models showing change of the same sign is required for this test to be significant.

The second test, displayed in the central column in the figures below was based on the hypothesis that the mean percentage change over the set of models is zero i.e. as a set, there is no change between the 20th century and the future scenario. This may be determined with a one-sample t test using the model percentage changes as our dataset, with an '*' indicating significance of this change at the 5% level.

The final test examined the number of individual models where there was a significant change in the mean daily occurrence of a particular synoptic type. The 5% level of significance was determined using the Livezey-Chen method (Wilks 2011) to determine the global significance of the set of individual model two-sample t tests. This is based on a binomial distribution with sample size M (the number of models) and the probability of occurrence of a significant result p = α = 0.05 where α is the local level of significance (i.e. that used for the individual test). Typically, the global significance level (i.e. the significance level of the binomial test) is also taken to be α .The plots show the number of significant models as a percentage of the total number of models (13 for SRESA2, 12 for SRESB1). An 'x' indicates global significance at the 5% level. Note that for 13 models (SRESA2) if we have ≥ 3 significant test results then this indicates global

significance at 0.0245 < 0.05. For 12 models (SRESB1) if we also have ≥ 3 significant test results then this indicates global significance at 0.0196 < 0.05.

June, July

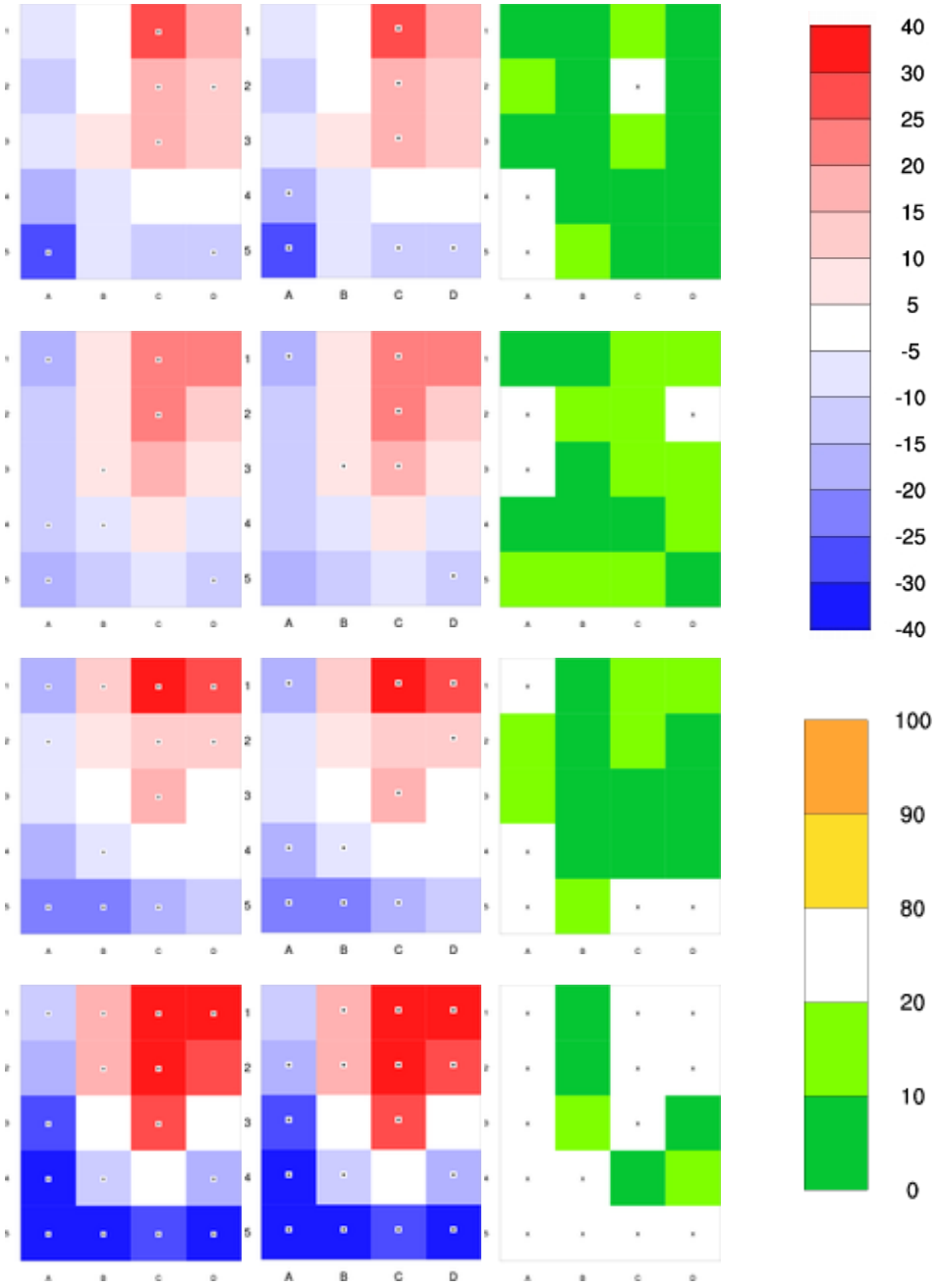

Figure 11 - JJ change. These plots show the mean percentage change in the daily occurrence of each synoptic type for the June and July SOM. The first row is 2045-65 minus 1961-2000 under the SRES B1 scenario; second row is 2045-65 minus 1961-2000 under the SRES A2 scenario; third is 2081-2100 minus 1961-2000 under the SRES B1 scenario and the bottom row is 2081-2100 minus 1961-2000 under the SRES A2 scenario. The plots with a red-blue scale show the mean percentage change. Overlaid on these plots are two tests of the significance of

this change .Left column: Power et al., (2011) method; Middle column: t-test. The right column shows the percentage of individual models with significant change between the present and the future; a star denotes significance.

It is clear in Figure 11 that the three different measures of significance of the multi-model mean generally align. Also, as more models agree on whether there has been an increase or decrease in the occurrence of a particular synoptic type (left column), more individual models also show significant changes (right column) and the overall strength of a change of zero also increases (central column). This strengthening certainty increases as the levels of greenhouse gases increase from the B1 to the A2 scenarios and from mid-century to the end of the century. One exception is the B1 scenario at mid-century, which shows far fewer deep low pressure systems (bottom left synoptic type) as compared to the present – fewer even than the A2 scenario or the B1 scenario at the end of the century. This aligns with the rapid reduction in SWWA rainfall under the B1 scenario as shown in Hope (2006). It is not clear why models project this rapid drying, although it is now clear that it is due to a strong decrease in the number of deep lows of this particular type. At the end of the century, rainfall levels are still low under the B1 scenario (Hope, 2006), but this is due to more highs and fewer lows of all types.

At the end of the century under the A2 scenario (bottom row of Figure 11) there is a strong, consistent signal. There will be more synoptic types with strong highs, and fewer with strong lows reaching up into SWWA latitudes. Given the corresponding rainfall anomalies (e.g. Hope et al., 2006; IOCI3 Milestone report 1) it is highly likely that the west coast of SWWA will see further rainfall reductions during the June, July season. Along the south coast the signal is not as clear as some of the synoptic types in the top right of the SOM (D1 and D2) are projected to increase in frequency.

July-December

In the July to December SOM (Figure 12), the distribution of the change is not as distinct as for the June,July case. This is probably due to the wide range of seasons covered by the SOM in comparison to the June,July case. However, under enhanced forcing from greenhouse gases (bottom row of Figure 12) a strong signal has emerged. Like in the June,July case, types that display regions

of low pressure become less prevalent under future scenarios, while types with extensive regions of high pressure become more common. Interestingly, synoptic types that have regions of both high and low pressure such as types A3 (11) and A2 (6), show a decrease in their occurrence although they display a strong high in the Indian Ocean. Type 35, which was important during the year of low puerulus return of 2008 and has off-shore winds is projected to strongly increase in its occurrence. It occurs most often in July and August in the late 20th century, and continues to more commonly appear during winter under future scenarios.

With regards to the puerulus count, there are many contributing factors to their number in any one year. In 2008 there was a particularly common synoptic type (E7, 35) that intuitively would make sense to discourage settlement. This synoptic type has been projected to increase. However, the life-cycle is complex and other factors are involved. This study will be continued by WA Department of Fisheries (Nick Caputi), using the knowledge gained by the research funded under IOCI.

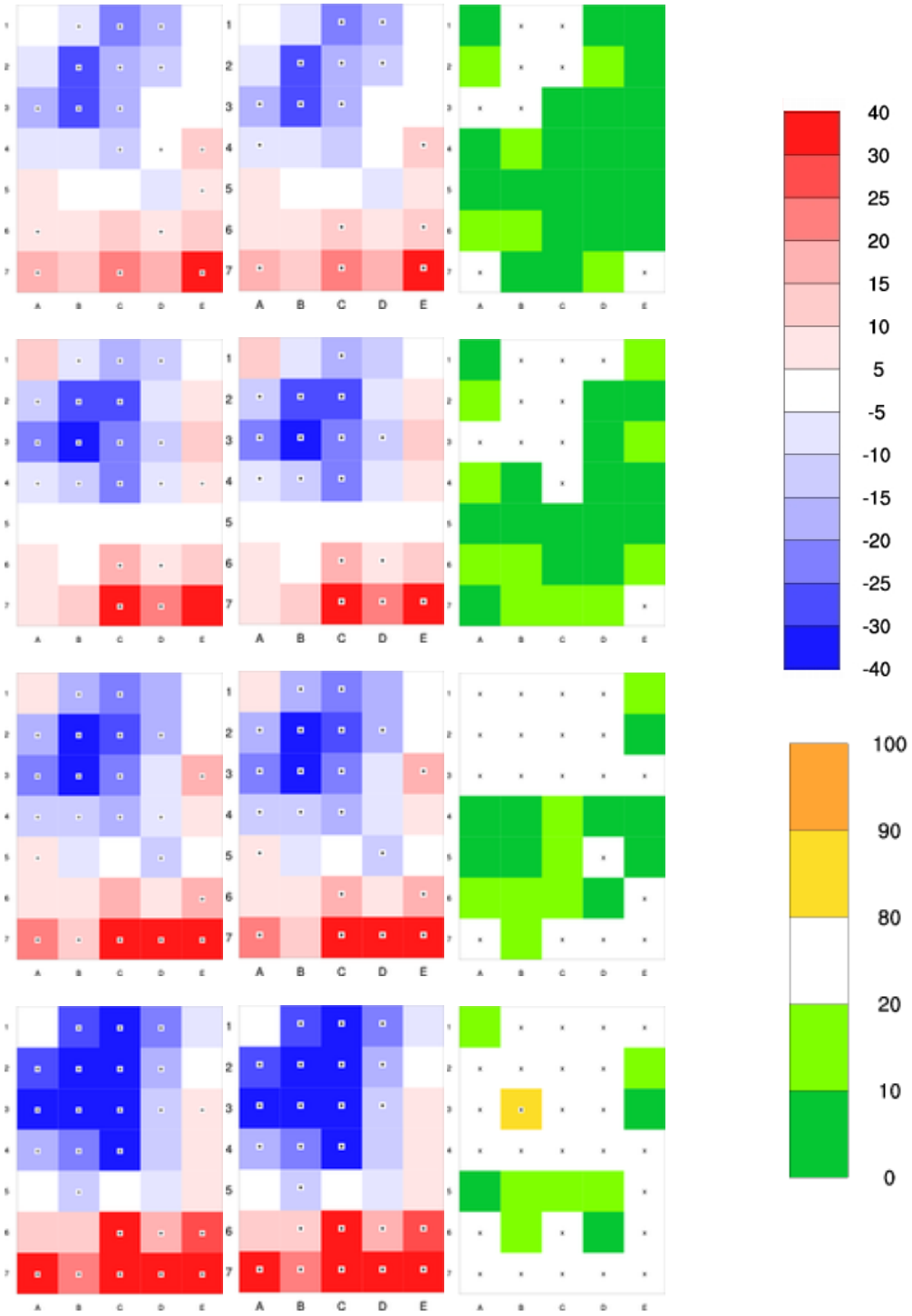

Figure 12 - JASOND change. The same as Figure JJ change, but for the July to December SOM.

January, February

The projected future conditions in summer (January and February) show distinct differences from the simulated present-day conditions even under relatively low levels of increased greenhouse gases (see top row of Figure 13). The synoptic

types (IOCI3 Milestones 2 and 3) that are projected to change the most tie in with the response in the June,July and July to December SOMs – types with high pressures increase in their occurrence while those with regions of deep low pressure decrease in their occurrence. The signal enhances as the levels of greenhouse gases increase and by the end of the 21st century.

If the pattern of the temperature anomalies associated with the types that are increasing in frequency (top left of SOM in Figure 14 - JF changes) is similar in the future, there will be more days conducive to cool conditions to the east of the south-west and along the coast (see IOCI3 Milestones 2 and 3). There will also be fewer days with warm conditions in that region. Along the west coast however, the opposite is true, with warmer conditions occurring more commonly. On the very south-west corner, changes are unclear. As the climate is not static, these circulation and temperature anomalies will probably be overlaid on a global upward trend in temperature. Thus, the west coast may warm more quickly than the global average, while conditions may not be as severe in the east of SWWA.

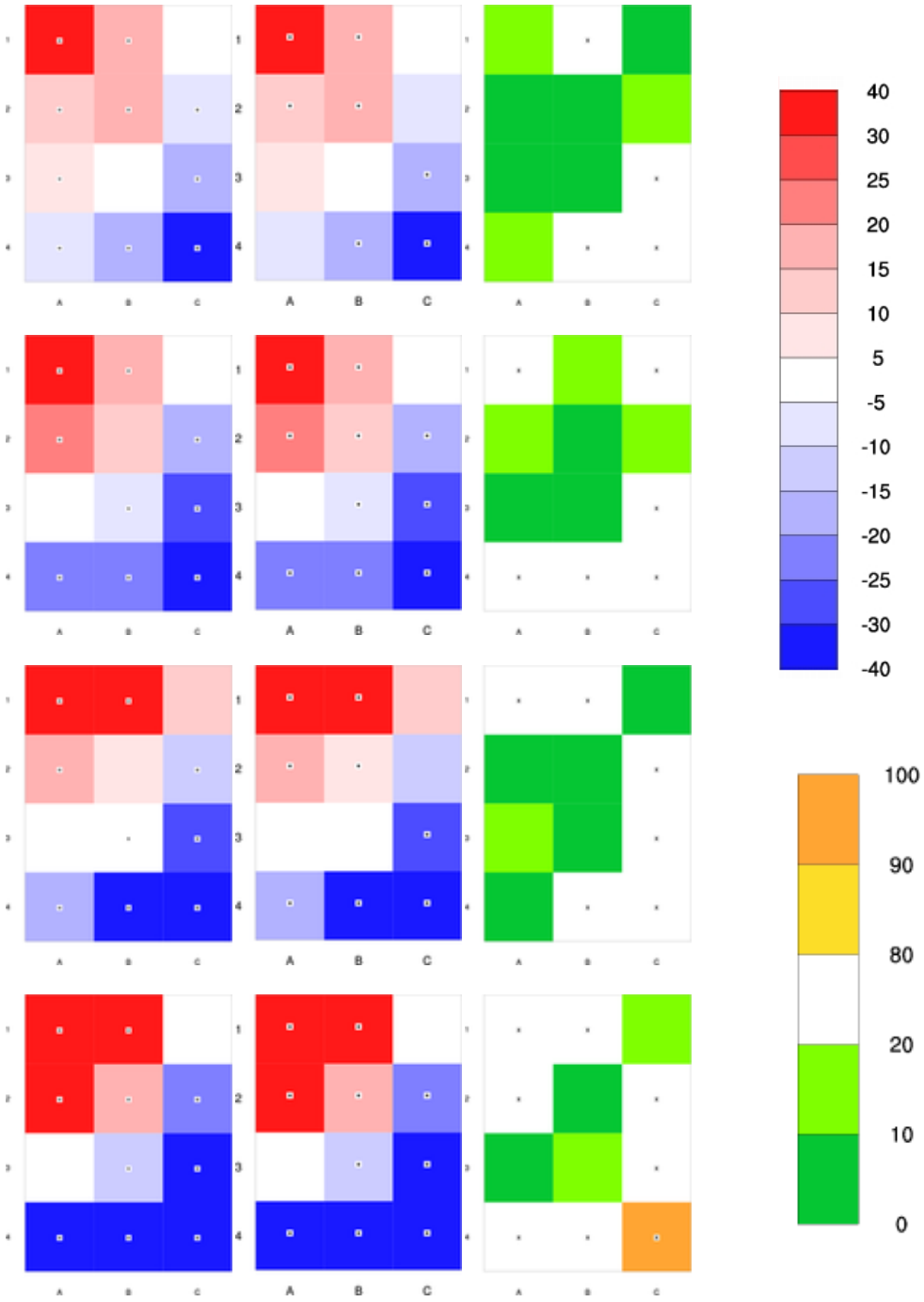

Figure 13 - JF change. The same as Figure JJ change, but for the January to February SOM.

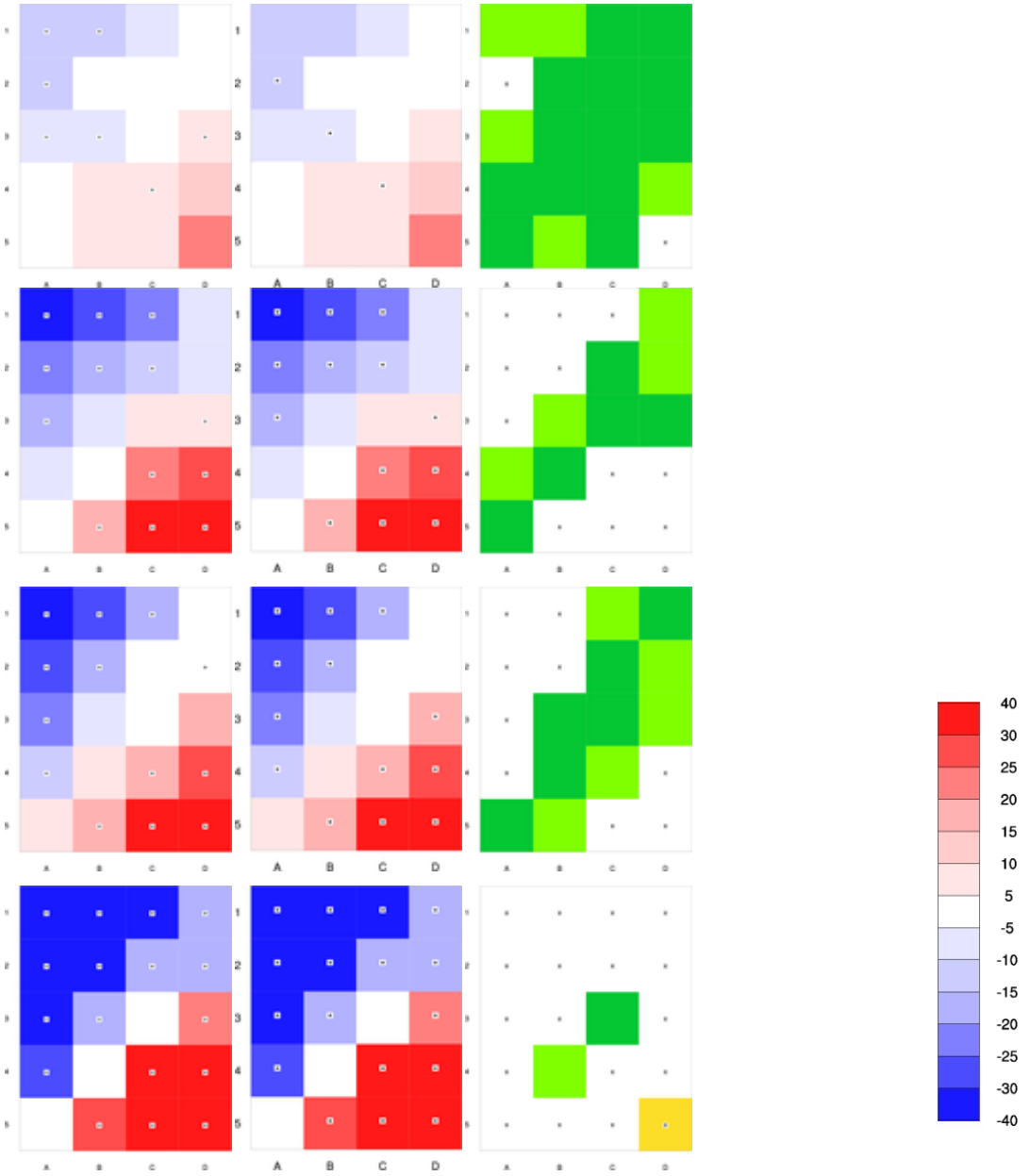

Figure 14 - MAM change. For the January to February SOM, the multi-model mean with a t-test significance test. SRES B1, mid-century differences on the left, then A2 mid-century, B1 end-of-century, then A2 end-of-century on the right.

March,April,May

The response simulated in March, April and May intensifies as greenhouse gas levels increase (Figure 14). Unlike the summer case, little change is seen under the B1 scenario at mid-century in autumn. However, under stronger greenhouse

gas forcing (A2 compared to B1), the signal is stronger and by the end of the century quite emphatic.

The SOM shown in the previous milestone report has synoptic types with a strong region of high pressure in the bottom right of the SOM. These, like in other seasons, are projected to increase in frequency. Synoptic types displaying a deep trough or trough to the west of the region, like in the winter SOM are also set to decrease in frequency under future projections. Both of these changes will likely continue to reduce the capacity for rainfall production across the SWWA.

Milestone 1.2.8 *Report on whether there is a clear link between the frequency of particular weather systems and the isotopic ratio of rainfall collected over the last 40 years*

Background

To gain an appreciation of the past decadal variability of the climate of the south-west, understanding can be gained from annually resolved proxies such as speleothems (cave stalagmites). Some of these, sourced from caves in the far south-west of the state, extend back tens of thousands of years (Treble, pers. comm. 2012). The isotopic ratio $^{18}O/^{16}O$[1] within the calcite layers of these stalagmites can preserve that of the rainfall when it fell in the past. However, the oxygen isotopes of rainfall itself are influenced by a number of factors that are site specific and must be understood before the proxy records can be accurately interpreted.

At this latitude, Treble et al. (2005b) discovered that local temperature variations have little bearing on the variations of oxygen istotopes in rainfall, and that they do represent variations in the rainfall amount.

The signature of oxygen isotopes in rainfall is strongly dependent on the total amount of rainfall per event, with more negative values of δ18O often associated with greater rainfall totals (the amount effect). However, the source region can

[1] ^{18}O is oxygen with 2 more neutrons than the far more common ^{16}O. It is thus heavier and behaves differently during changes of state from gas to liquid or vice versa. At each change the heavier isotope is concentrated in the liquid compared to the gas. The ratio $^{18}O/^{16}O$ is expressed as $\delta^{18}O$ and near the equator is near zero, near the poles the isotopes are depleted of ^{18}O, are lighter, and the ratio can be as low as -20‰

also alter the ratio, as noted in the footnote below, and described by Treble et al., 2005a for Tasmania.

Given these associations, it was believed that the GNIP (Global Network Isotopes in Precipitation) rainfall isotope data (1962-1976, 1983-2000) from Perth could be used along with our understanding of the circulation influencing SWWA gained through IOCI to develop a robust relationship between δ18O and source to derive total rainfall. Fischer and Treble (2008) have since gone a good way to describing that indeed a circulation parameter can provide key detail to the link between δ18O records and total rainfall. They found a particular pressure pattern that dictates the direction of flow onto the SWWA domain was very important in determining whether a high value of δ18O is due to low rainfall totals or a shift in the circulation to a more tropical source. They found that during the period of low rainfall since the late 1960s, values of $\delta^{18}O$ have been high, as expected from the amount effect. However, during the period 1930-1955, a period of high rainfall, $\delta^{18}O$ was also high. This was found to be because the circulation pattern had switched to bringing moisture from a more tropical, and hence higher $\delta^{18}O$ value, source.

To extend the work of Fischer and Treble (2008), new daily rainfall isotope data has allowed a finer scale analysis of the synoptic situations associated with each rainfall event over the last five years.

Data and Method

Pauline Treble, with assistance from staff at Calgardup Cave, has measured daily rainfall totals and rainfall oxygen and hydrogen isotopes for the last five years from a site above Calgardup cave (-34.05S 115.03E decimal degrees). Although this record is short, it encompasses the south-west's driest years on record (2006 and 2010) and two relatively wet years (2008 and 2009) (see Figure 15). It is clear that Calgardup cave is located in a wet part of the south-west. The data was limited to the wettest two months of the year: June and July, when rainfall declines have also been observed since the late 1960s (IOCI 2002).

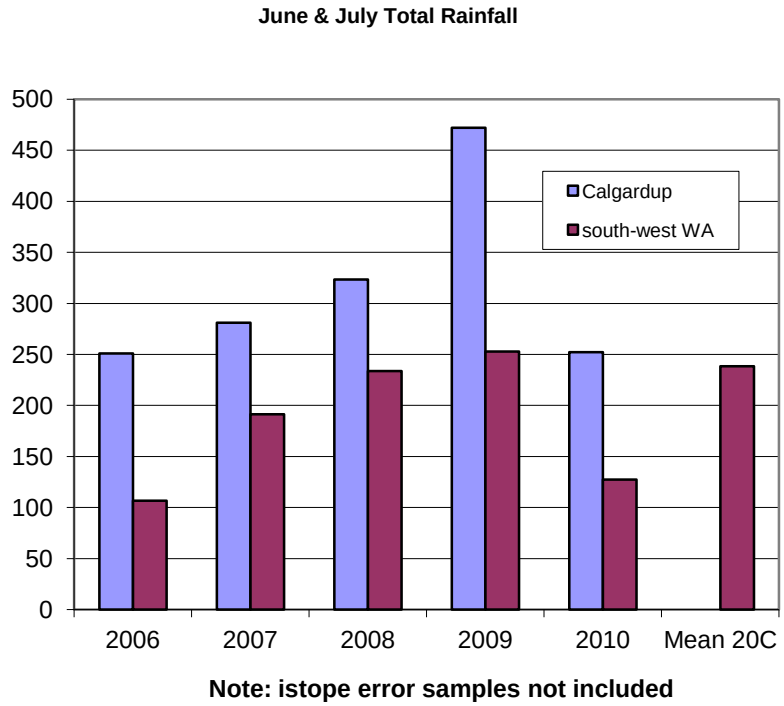

Figure 15. Total June and July rainfall for each of the five years 2006-2010. For site above Calgardup cave and for the averaged south-west WA region using Bureau of Meteorology gridded data (Jones et al., 2009).

Both back trajectory analysis and self-organising maps were used to explore the synoptic situation associated with each rainfall event. The back trajectories were run by Alan Wain through weather forecast datasets from the Bureau of Meteorology archive for four days preceding each rain event. The self-organising map used was the June,July SOM reported on in IOCI3 milestone report 1.

Results

The back trajectory analysis revealed that there are indeed quite distinct source regions from event to event. Two examples are described here. Figure 16 shows a case on the left where the source is uniformly from the south of the region for all levels on the day of the event. This day corresponded to synoptic type D1 in the June, July SOM (see Figure 17, top right). On the days preceding the event, the SOM types would likely have been moving in an anti-clockwise progression around the edge of the SOM (Types D3, D2, then D1). (Hope et al. (2006) describe the likely progression of types within this SOM). It is thus clear why southerly flow would precede a day fitting this synoptic type. On the right of

Figure 16 the source is more local, and derives from the west or north-west of the region. The SOM type is number A2. Again, following the probable synoptic types anti-clockwise around the SOM in the days preceding the event (types A1, B1), it is clear that these align with the resultant track. It is thus plausible that the SOM pattern on a day or two preceding the event will better constrain the source aspect of the $\delta^{18}O$ value. Together these two methods provide an intuitive description of the source for each event, which will be explored further in Hope et al. (2013).

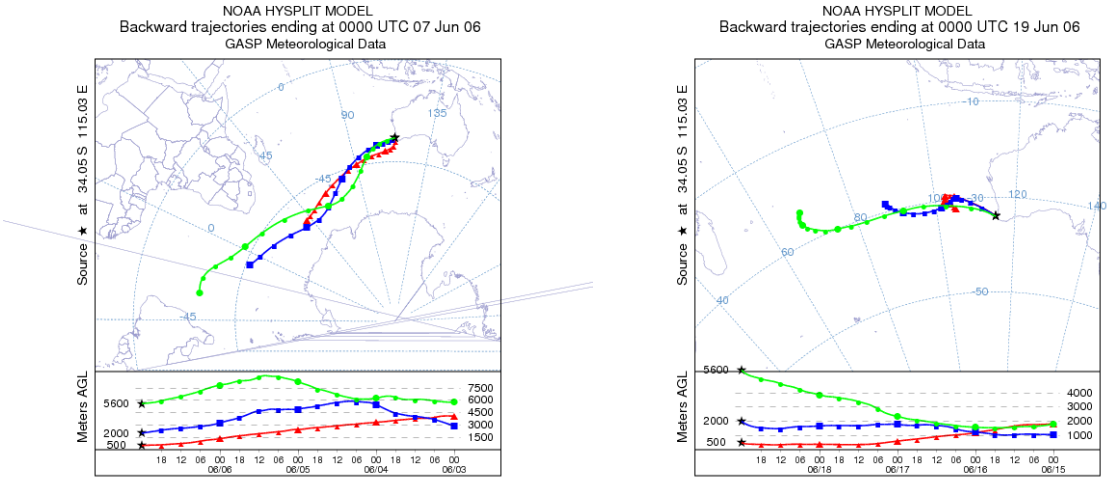

Figure 16 - traj. Four day back trajectories from rainfall events at Calgardup cave showing differing source directions. Left panel shows a source from the south, while the right panel shows a source from the north-west.

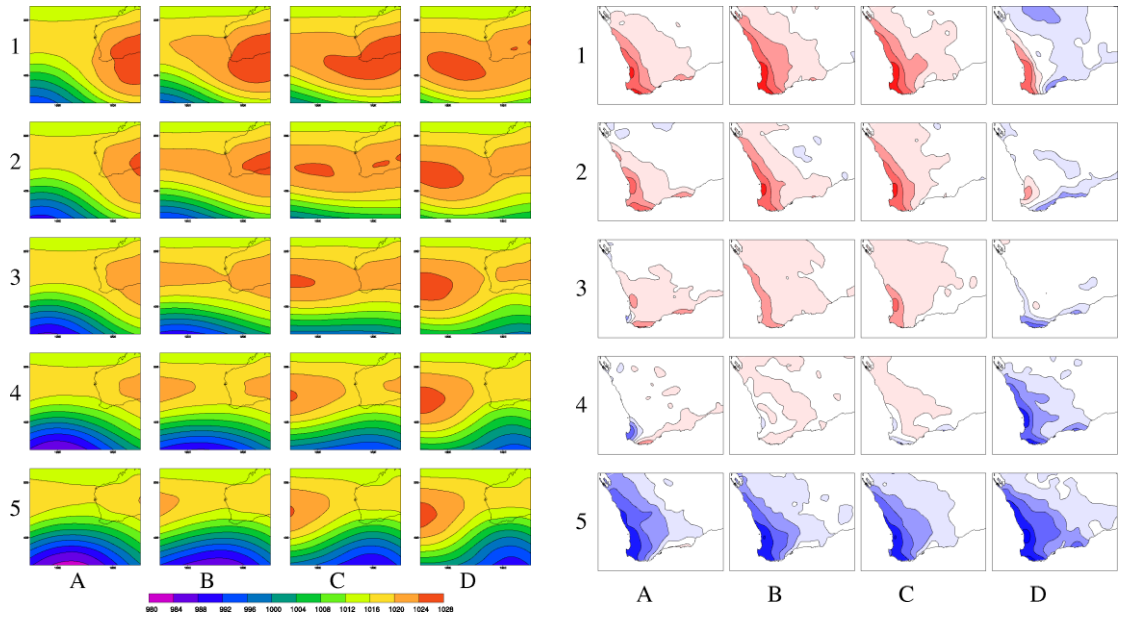

Figure 17 - JJ SOM On the left is the 4 by 5 SOM built using 1948 to 2003 NCEP/NCAR reanalyses MSLP showing the continuum of June and July weather systems that impact SWWA. The reds indicate high pressure and the blues lower pressure. References to individual synoptic types in the text are to, for example, A5, which is the bottom left type. Contour interval is 4 hPa

On the right is the NCC 0.25x0.25 degree gridded rainfall anomalies associated with each type in the 4 by 5 SOM. Red shading indicates conditions drier than the 1958–2003 mean and blue wetter than the mean. The contour interval is variable: -8, -4, -2, -1, -0.3, 0.3, 1, 2, 4, 8 mm/day. From:Hope et al., 2006.

The association between $\delta^{18}O$ and the square root of rainfall above Calgardup cave (Figure 18) shows that there is a negative association, showing that the rain amount effect is evident. After combining the two wet years and the two dry years (as seen across the wider south-west) the effect is still evident, with lower $\delta^{18}O$ values for the wetter years and higher values for the drier years.

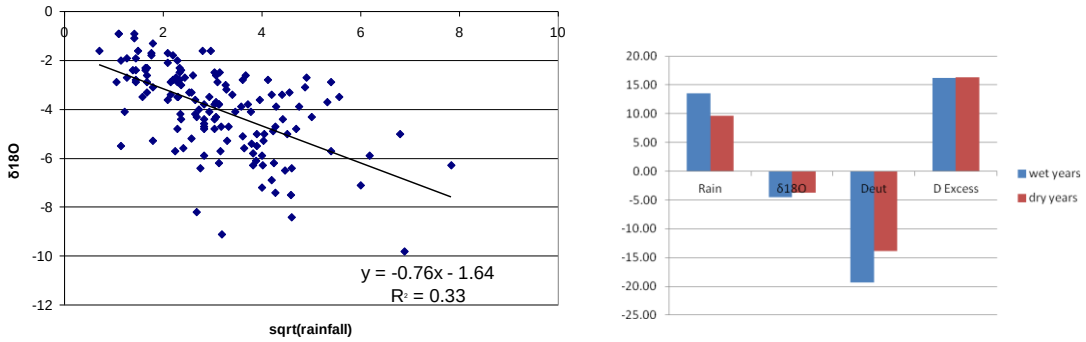

Figure 18 - rain 18O. Left panel shows the association event by event between the square root of rainfall (mm) and $\delta^{18}O$ with a linear fit drawn. The right panel shows the totals of rainfall, $\delta^{18}O$, deuterium and deuterium excess for the two wet years (in blue) and dry years (in red) over the five year period.

Event by event there is variability in the circulation associated with any one rainfall day. However, grouping the two dry years (as seen across the wider south-west), and the two wet years of these five years of isotope data reveals a clear signal as to the dominant circulation type during those times. The dry years have a far greater representation of types in the top right-hand of the SOM which are dominated by a region of high pressure extending from the southern Indian Ocean to the continent. From the trajectory analysis, it was seen that this is often associated with southerly flow. In wet years, rainfall events arise predominantly from synoptic types with deep troughs extending up over the region from the south, with source regions to the north-west (the preceding days would have types in the left-hand side of the SOM, e.g. types A3 or A4).

These results confirm the confounding characteristics of the rainfall regime influencing this corner of SWWA. High rainfall events often draw on rainfall deriving from the north-west of the region (Wright, 1974; Hope et al., 2006). Thus there will be a high $\delta^{18}O$ signature from the tropical source, but a low $\delta^{18}O$ signature from the rain-out effect due to the high rainfall total. Low rainfall events at this location often derive from post-frontal rainfall or rainfall along the south-coast, with a southerly flow. Conversely to high rainfall events, there will be a low $\delta^{18}O$ signature from the southerly source, but a high δ18O signature due to a limited rain-out effect.

Milestone 1.2.9

If 1.2.8 is successful and time and funding are sufficient, report on probably time series of weather systems as suggested by the isotopic ratios in cave structures to place the current rainfall changes in context.

One limitation in the analysis done for Milestone 1.2.8 is that the circulation data required to interpret the rainfall totals derived using speleothem $\delta^{18}O$ were from the instrumental record. In order to reconstruct long series extending back before the instrumental record, there must be alternative methods by which to gain a sense of the dominant circulation at a time of high $\delta^{18}O$ values.

One possible source of guidance can be gained from other isotopic data from the speleothems. Deuterium excess (a measure of the relationship between 'heavy' hydrogen and oxygen isotopic ratios) has been suggested as an indicator of the source region of rainfall (Uemura et al., 2008). Hydrogen isotopes in rainwater have until recently been more challenging to measure, but advances in laser spectroscopy techniques make routine measurement of large quantities of samples possible (Treble, pers. comm., 2012). If we found that it did indeed reveal something of the source of the moisture parcels in a rainfall event, we could have found both a measure of the rain amount in the $\delta^{18}O$ in the proxy indicator and the circulation type from the deuterium excess. We could thus have been able to reconstruct total rainfall from speleothems using coupled measurements of calcite $\delta^{18}O$ and water $\delta^{18}O$/dD. Unfortunately, in this case, there was no clear distinction between wet or dry years in terms of deuterium excess (Figure 19 - rain d18O), and the $\delta^{18}O$ or deuterium alone probably reveals more about the rainfall signature than the combined calculation of deuterium excess. This is not surprising given the very high correlation between $\delta^{18}O$ and deuterium at this site: r=0.96 for all events; 0.94 for dry years; 0.97 for wet.

It may be possible to achieve an estimate of the mean circulation conditions on a longer timescale by drawing on other proxies that hold information for SWWA. From the comprehensive analysis of Southern Hemisphere proxy records (Neukom and Gergis, 2011), there are three other records that may be of use to assess south-western Australia rainfall plus possible linkages to the Northern Hemisphere(Yun Li, pers. comm., 2012). The Southern Hemisphere records include the precipitation record from the Law Dome ice-core in eastern Antarctica

(van Ommen & Morgan, 2010), tree-ring records from near Esperance (Cullen and Grierson, 2009) and a coral record from the Abrolhos (Khunert et al., 1999). Each of these records is on the edge or completely outside of the region under consideration, thus the climatic connections and circulations that interact with these regions must be considered rather than a direct correlation with local south-west rainfall.

The Abrolhos are off-shore from Geraldton, and thus at the very northern extent of the south-west region. In their paper, Khunert et al. (1999) consider the record as an indicator of local sea-surface temperatures and the behaviour of the Leeuwin current. One interesting feature of this record is that "A long-term rise in temperature by 1.4 3C over two hundred years is inferred from the isotope record...". Analysis of the present-day interactions between temperatures in this region and south-west rainfall has been limited, and thus it is not entirely clear what this warming means for south-west rainfall.

Some studies have suggested that the waters in this region are key for the potential for moisture uptake in the pre-frontal airflow that is so important to rainfall along the west coast (England et al., 2006; Hope et al., 2006). However, this record of sea temperature will not reflect larger changes to the number deep low pressure systems through time (for example, discussion in IOCI3 projects 1.1 and 1.2; Hope et al., 2006).

The tree-ring records are drawn from trees near Esperance, at the eastern extent of the south-west region (Cullen and Grierson, 2009). This record has been discounted by van Ommen and Morgan (2010) because it is so far east. Rainfall along the southern coast and to the east of the region did not experience the same rainfall declines as along the west coast in the late 1960s (Hope et al., 2006), and thus the rainfall variability in this region can indicate a different circulation type from those impacting the west coast. However, correlations of this record with winter rainfall (Bureau of Meteorology gridded data) during their period of overlap (1911-2005) by Joelle Gergis reveal surprisingly consistent correlations over the region (Figure 19). Given that we know that rainfall in this region and the south-west can be vary in concert or differently depending on the circulation type, a combination of these two records may reveal something about

the dominant large-scale circulation of the period, but this would require a great deal more analysis.

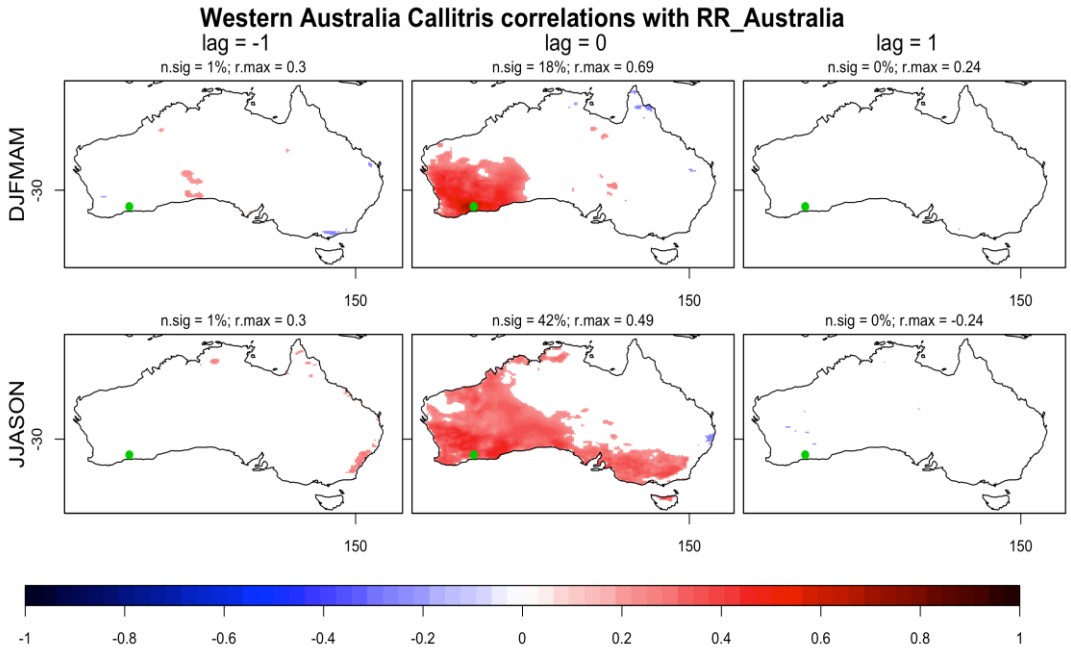

Figure 19 - raincortee. From Aus2K conference, Perth, 2012, Gergis: Correlations between tree ring data and gridded rainfall at -1, 0 and 1 year lag for each half year

In order to gain an appreciation of the broader circulation changes impacting SWWA, van Ommen and Morgan (2010) suggest that precipitation rates at Law Dome in eastern Antarctica show correlations with rainfall in SWWA and describe plausible mechanisms for this to be the case. They noted that "The precipitation anomaly of the past few decades in Law Dome is the largest in 750 years, and lies outside the range of variability for the record as a whole...". This result suggests that the circulation changes that have driven the rainfall declines in SWWA (e.g. IOCI Milestones 1.1 and 1.2) and that have been noted as unusual in the 55 years of reliable reanalyses data are also unusual in a far longer context. However, the Law Dome precipitation record shows high precipitation rates during the unusual 1930-1955 period in the speleothem $\delta^{18}O$ records which would usually be associated with dry conditions in SWWA. Thus it too is an index that, like all the others, requires an appreciation of its strengths and limitations. This further understanding may be gained by combining the proxy records from a

number of sources with an understanding of present-day circulation patterns. However, that study is well beyond the scope of the IOCI3 work.

References for all milestone reports under subproject 1.2

Cullen, L. E. and P. F. Grierson, 2009: Multi-decadal scale variability in autumn-winter rainfall in south-western Australia since 1655 AD as reconstructed from tree rings of Callitris columellaris. Climate Dynamics, 33, 433-444.

England, M. H., C. C. Ummenhofer, and A. Santoso, 2006: Interannual rainfall extremes over southwest Western Australia linked to Indian Ocean climate variability. Journal of Climate, 19, 1948-1969.

Fischer, M. J. and P. C. Treble, 2008: Calibrating climate-δ18O regression models for the interpretation of high-resolution speleothem δ18O time series. Journal of Geophyscial Research, 113, D17103.

Hope, P., P.C. Treble, M.J. Fischer and A. Wain, 2013: A multi-faceted approach to describe the circulation impact on event-based rainfall δ18O. In preparation.

Hope, P. K., 2006: Projected future changes in synoptic systems influencing southwest Western Australia. Climate Dynamics, 26, 765-780.

Hope, P. K., W. Drosdowsky, and N. Nicholls, 2006: Shifts in synoptic systems influencing south west Western Australia. Climate Dynamics, 26, 751-764.

Jones, D. A., W. Wang, and R. Fawcett, 2009: High-quality spatial climate data-sets for Australia. Australian Meteorological and Oceanographic Journal, 58, 233-248.

Kalnay, E., M. Kanamitsu, R. Kistler, W. Collins, D. Deaven, L. Gandin, M. Iredell, S. Saha, G. White, J. Woollen, Y. Zhu, M. Chelliah, W. Ebisuzaki, W. Higgins, J. Janowiak, K. C. Mo, C. Ropelewski, J. Wang, A. Leetmaa, R. Reynolds, R. Jenne, and J. D, 1996: The NCEP/NCAR 40-Year Reanalysis Project. Bulletin of the American Meteorological Society, 77, 437-471.

Kuhnert, H., J. Patzold, B. Hatcher, K.-H. Wyrwoll, A. Eisenhauer, L. B. Collins, Z. R. Zhu, and G. Wefer, 1999: A 200-year coral stable oxygen isotope record from a high-latitude reef off Western Australia. Coral Reefs, 18, 1-12.

Meehl, G. A., C. Covey, T. Delworth, M. Latif, B. McAvaney, J. F. B. Mitchell, R. J. Stouffer, and K. E. Taylor, 2007: The WCRP CMIP3 multi-model dataset: A new era in climate change research,Bulletin of the American Meteorological Society, 88, 1383-1394.

Neukom, R. and J. Gergis, 2011: Southern Hemisphere high-resolution palaeoclimate records of the last 2000 years. The Holocene, in press.

Power, S., F. Delage, R. Colman, and A. Moise, 2011: Consensus on 21st century rainfall projections in climate models more widespread than previously thought. Journal of Climate, in press.

Taylor, K. E., R. J. Stouffer, and G. A. Meehl, 2012: An overview of CMIP5 and the experiment design Bulletin of the American Meteorological Society, 93, 585-498, doi:10.1175/BAMS-D-11-00094.1 <dx.doi.org/10.1175/BAMS-D-11-00094.1>

Treble, P. C., W. F. Budd, P. K. Hope, and P. K. Rustomji, 2005a: Synoptic-scale climate patterns associated with rainfall δ18O in southern Australia. Journal of Hydrology, 302, 270-282.

Treble, P. C., J. Chappell, M. K. Gagan, K. D. McKeegan, and T. M. Harrison, 2005b: In situ measurement of seasonal δ18O variations and analysis of isotopic trends in a modern speleothem from southwest Australia. Earth and Planetary Science Letters, 233, 17-32.

Uemura, R., Y. Matsui, K. Yoshimura, H. Motoyama, and N. Yoshida, 2008: Evidence of deuterium excess in water vapor as an indicator of ocean surface conditions. Journal of Geophyical Research, 113, D19114, doi:10.1029/2008JD010209.

van Ommen, T. D. and V. Morgan, 2010: Snowfall increase in coastal East Antarctica linked with southwest Western Australian drought. Nature Geoscience, 3, 267-272.

Wilks, D.S, 2011: Statistical Methods in the Atmospheric Sciences, 3rd Ed., Elsevier, Amsterdam, 676 pp.

Summary of new linkages to other IOCI3 Project

Nil

Summary of any new research opportunities that have arisen

The frontal analysis work continues in the background, and we hope to gain funding to progress this further.

Our results contribute to a study by Nick Caputi.

Alterations to research plans

Introduce an analysis of temperatures for the summer synoptic analysis.

List of Publications Accepted and Submitted

Hope, P. and C. J. Ganter, 2010: Recent and projected rainfall trends in south-west Australia and the associated shifts in weather systems. In: Book of Proceedings from Greenhouse 2009 Conference, I. Jubb, P. Holper, and W. Cai, Eds., CSIRO Publishing.

Braganza, K., S. Power, B. Trewin, J. Arblaster, B. Timbal, P. Hope, C. Frederiksen, and J. McBride, 2011: Update on the state of the climate, long-term trends and associated causes. In: *Climate science update: A report to the 2011 Garnaut Review. CAWCR Technical Report* ***36***.T. D. Keenan and H. A. Cleugh, Eds., The Centre for Australian Weather and Climate Research, 107 pp.

List of IOCI-Related Presentations at National of International Conferences, Symposia and Workshops

Hope, P. and C.J. Ganter, 2010: South west Western Australia summer temperature cooling trend. Australia and New Zealand Climate Forum, Hobart

Hope, P., K. Keay and C.J. Ganter, 2012: Using a Self-Organising Map to capture the range of current and future weather systems. AMOS annual conference, Sydney

Hope, P., K. Keay, M. Pook, J. Catto, I. Simmonds, G. Mills, P. McIntosh, J. Risbey and G. Berry, 2012: Objective methods of frontal recognition – a case study in south western Australia. AMOS annual conference, Sydney

Summary of Progress Status

Complete

Appendix

Milestone 1.2.6 *Report on whether these systems are expressed in climate model simulations.*

June & July

There are no synoptic types as represented by the NCEP/NCAR reanalyses (NNR) SOM that are not present in any model simulation of the late 20th century (1961-2000), see Figure A1. There is however, one type that is consistently less well-represented in five of the 13 models, D5. D5 displays an intense high in the Indian Ocean and a very deep trough to the south of WA. Model **b** (CNRM-CM3) displays a different pattern of variability across the synoptic types than NNR, with fewer of the extreme types and more of the types close to the mean, however all are still represented.

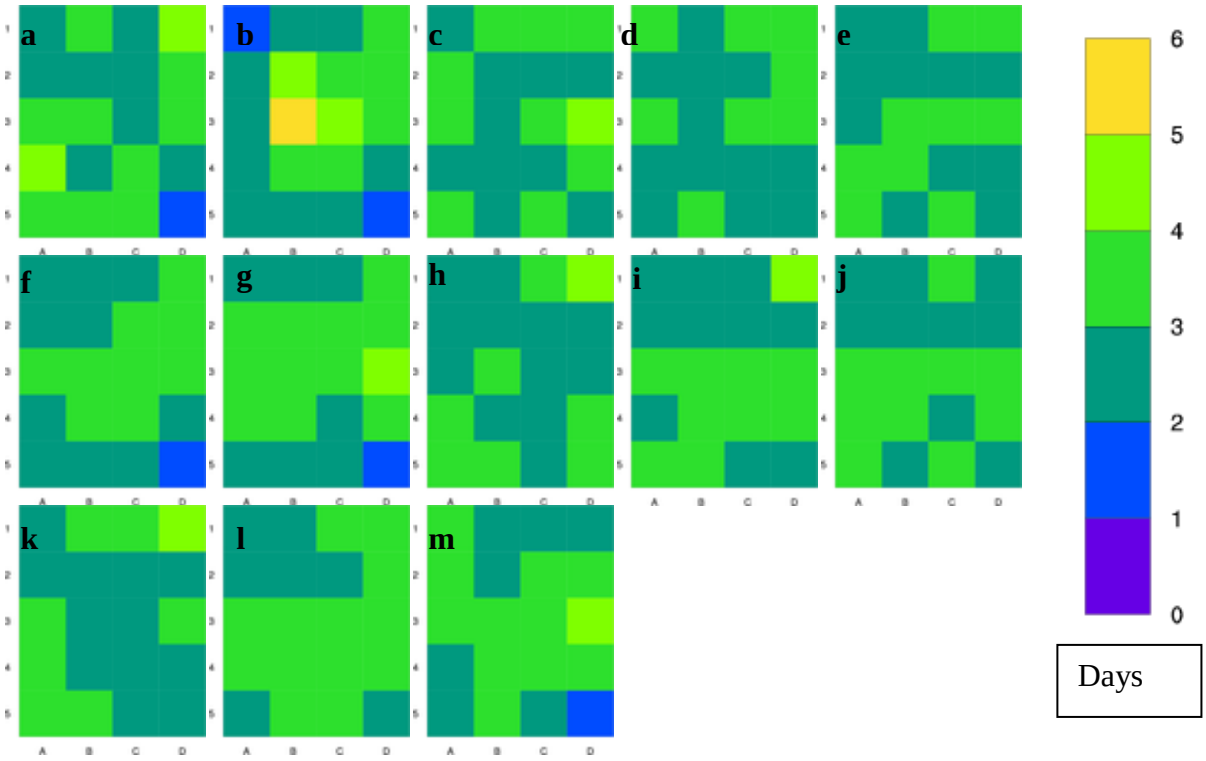

Figure A1. The counts of each synoptic type in the June and July SOM for each climate model (see Table 1). The raw count has been standardized to represent the number of days per season – in this case 61. An even distribution would have 61/20 ≈ 3 days per synoptic type

July, August, September, October, November, December

All models

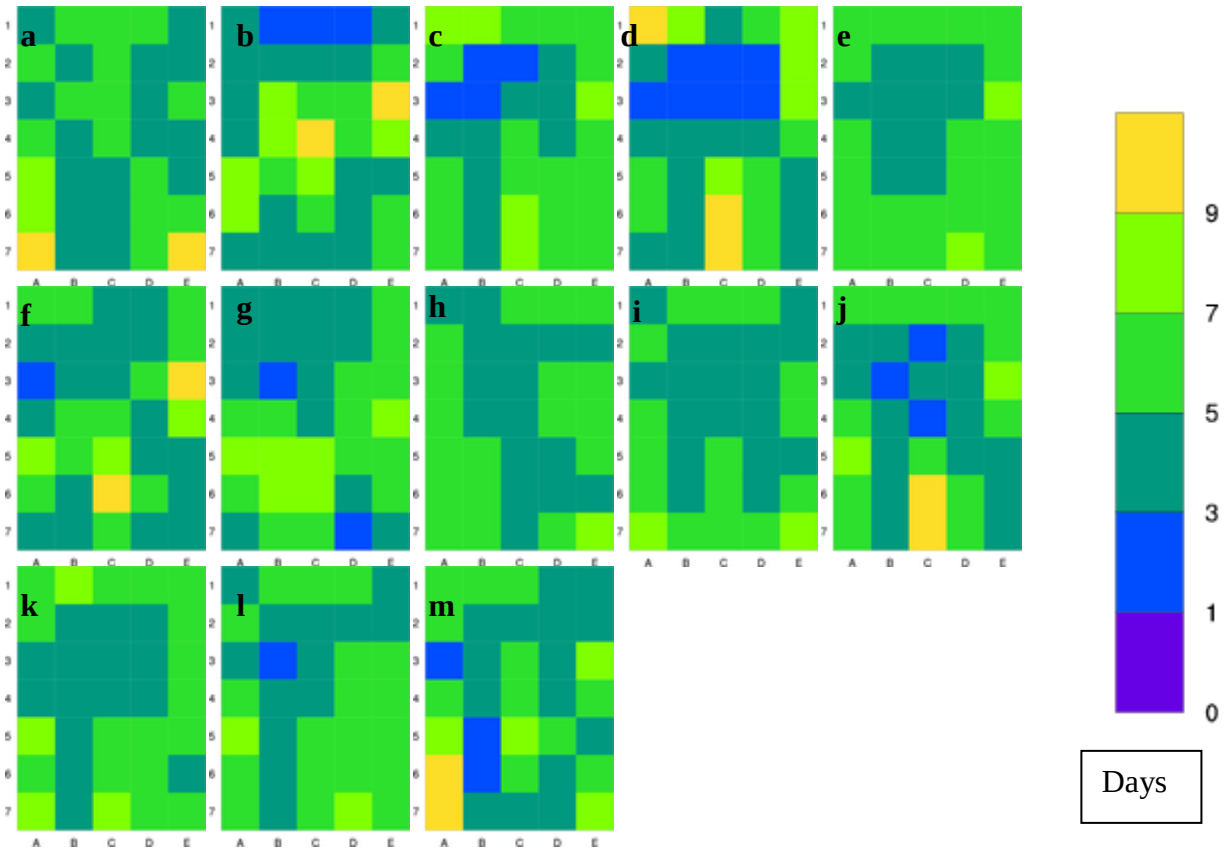

Figure A2. The counts of each synoptic type in the July to December SOM for each climate model (see Table 1). The raw count has been standardized to represent the number of days per season – in this case 184. An even distribution would have 184/35 ≈ 5 days per synoptic type

January, February

All models display a reasonably even representation of each synoptic type (Figure A3). Only model **a** has a type that is less commonly represented. However all models simulate all synoptic types represented by NNR in their late 20th century simulations.

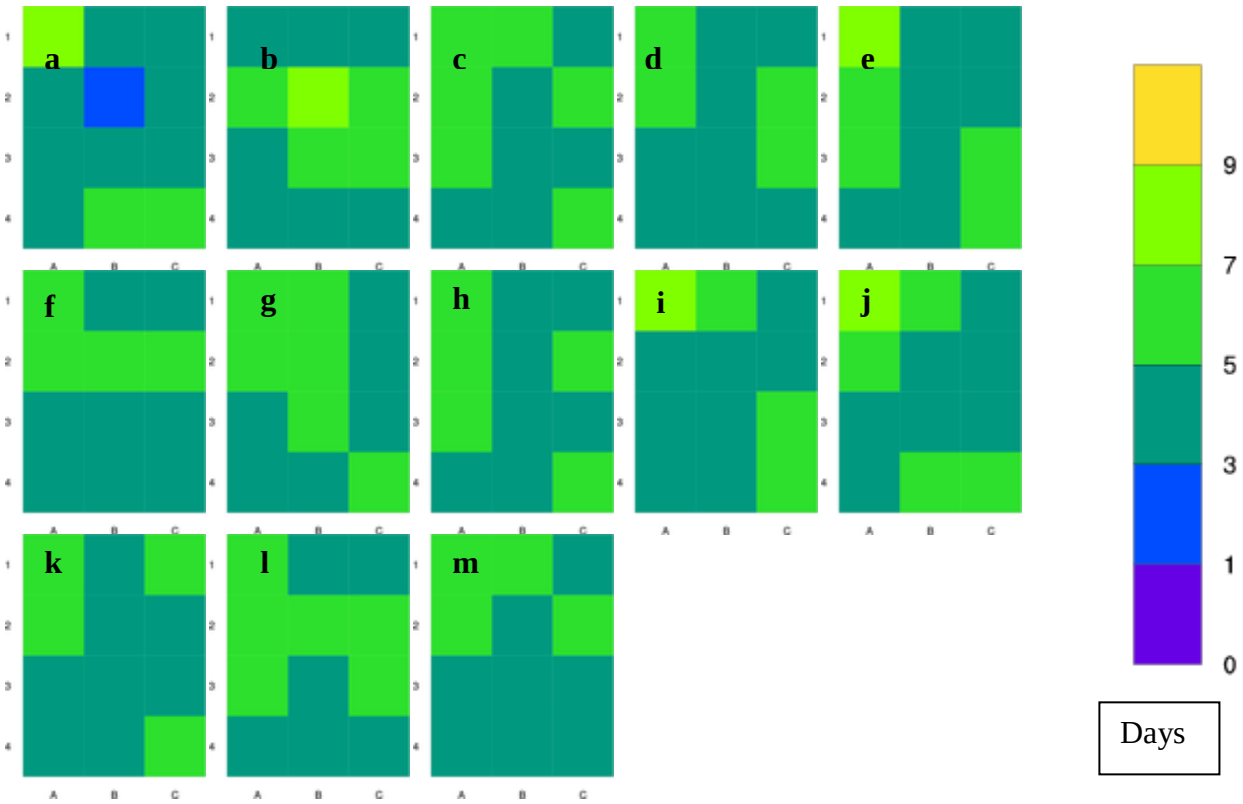

Figure A3. The counts of each synoptic type in the January and February SOM for each climate model (see Table 1). The raw count has been standardized to represent the number of days per season – in this case 59. An even distribution would have 59/12 ≈ 5 days per synoptic type

March, April, May

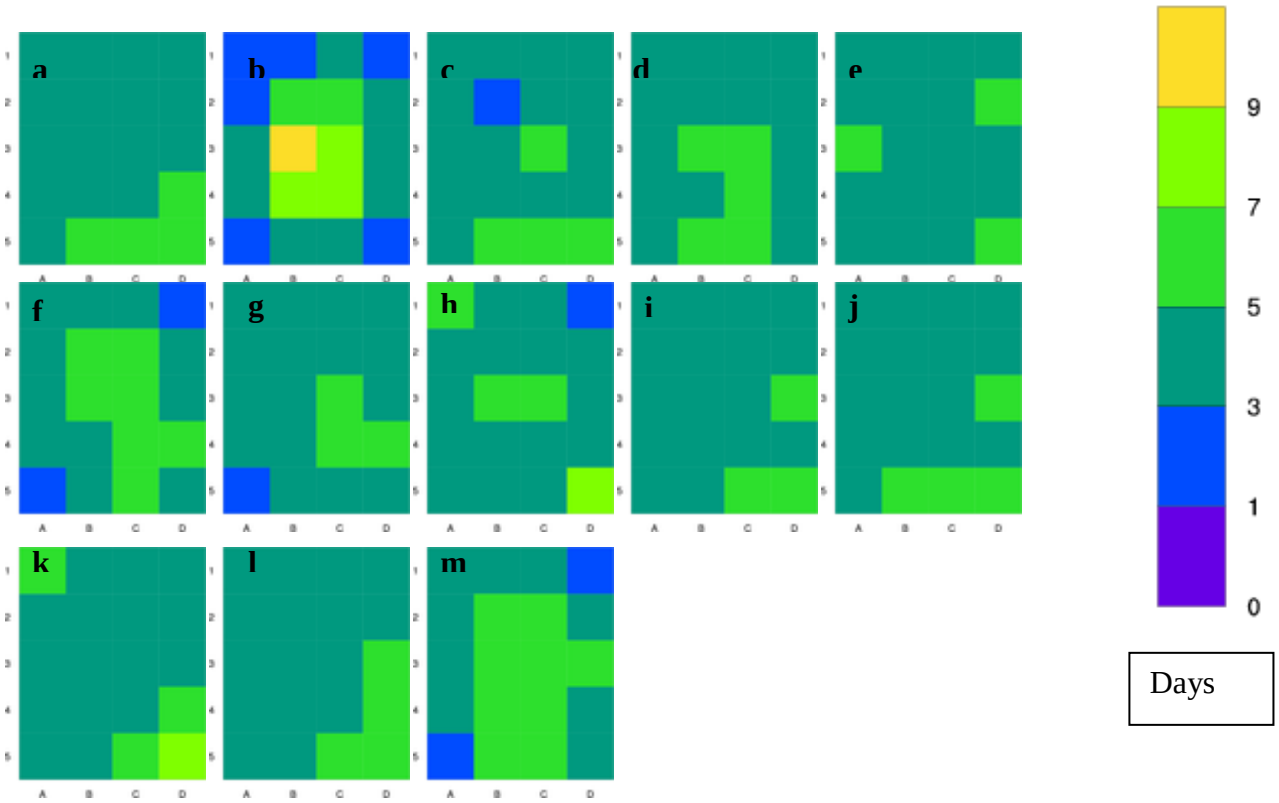

Figure A4. The counts of each synoptic type in the March, April and May SOM for each climate model (see Table 1). The raw count has been standardized to represent the number of days per season – in this case 92. An even distribution would have 92/20 ≈ 4.6 days per synoptic type.

Milestone 1.2.7 *Report on whether these systems change in frequency in simulations of future scenarios.*

June & July

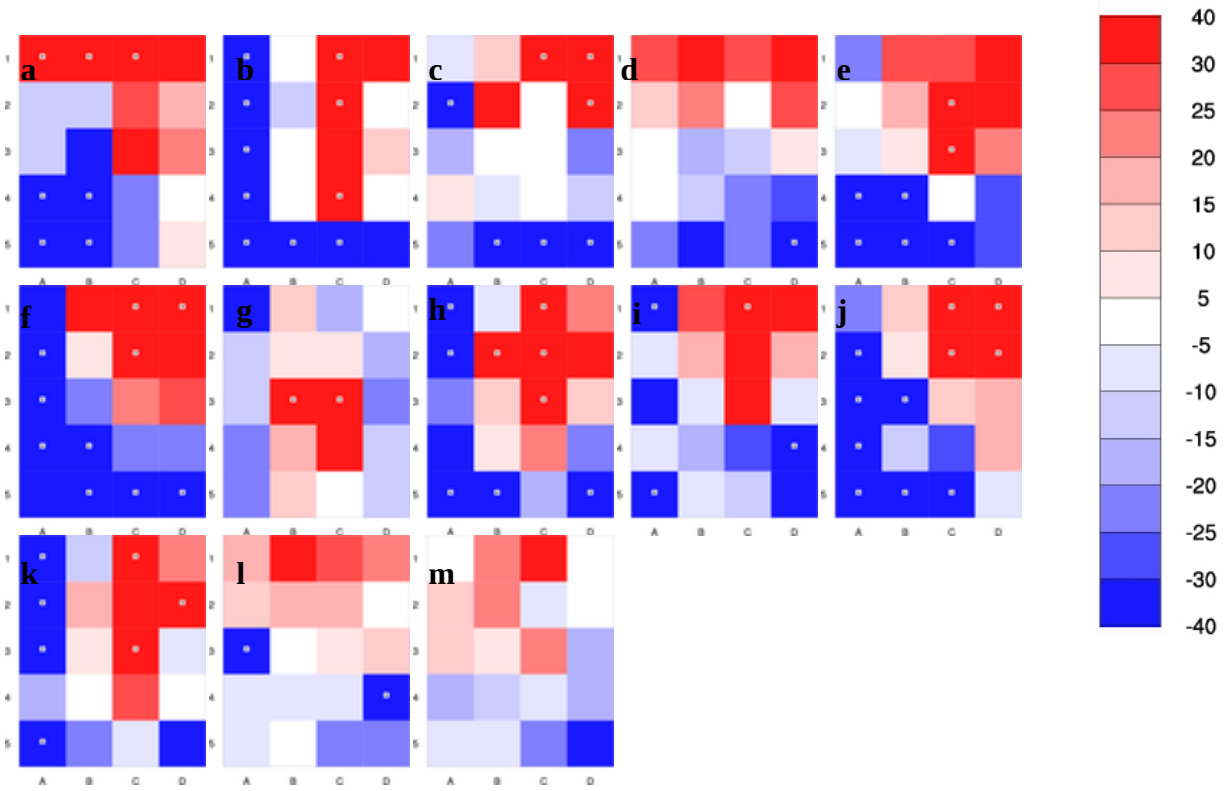

Figure A5 - models ttest. The percentage change of the daily occurrence of each synoptic type between 2081-2100 and 1961-2000. Significance is calcualted using an unpaired t-test and an '*' indicates significance of this change at the 5% level.

PROJECT 1.2: South-West Western Australia's Regional Surface Climate and Weather Systems

Principal Investigator(s): *Dr Pandora Hope, Kevin Keay and Catherine J. Ganter*

To be Completed for First Annual Report, and Included in Subsequent Annual Reports		To be Completed for First Annual Report and Updated in Subsequent Annual Reports	
Milestone description[1]	Target completion date[2]	Progress[3] against milestone (1- 3 dot points)	Recommended changes to research plan[4] (1- 3 dot points)
1.2.1 Note on the frequency of winter weather systems impacting the south-west in the last few years	31/12/2009	Achieved – a chapter for a book from the Greenhouse 2009 conference	1. Additional methods of classifying particular types of weather systems (highs and troughs) were used and compared
1.2.2 a. Report on the rainfall variability and trends in all seasons. b. Has there been a shift in rainfall intensity over the last 40 years?	31/12/2009	Completed a. A poster was produced, and used at GH9, and by BoM WA office b. Results presented at IOCI workshop in Oct 2009.	Updated with AWAP

1.2.3 Report on the range of weather systems identified by the new classification scheme for south-west summer weather systems	31/12/2010	Completed	Linking synoptic patterns to summer temperatures
1.2.4 Report on range of weather systems identified by the new classification scheme for south-west spring and autumn weather systems	31/12/2010	Completed	
1.2.5 Report on the time series of these systems in the observations	31/12/2011	Complete	
1.2.6 Report on whether these systems are expressed in climate model simulations	31/12/2011	Complete	
1.2.7 Report on whether these systems change in frequency in simulations of future scenarios	31/12/2011	Complete.	
1.2.8 Report on whether there is a clear link between the frequency of particular weather systems and the isotopic ratio of rainfall collected over the last 40 years	31/12/2011	Complete, but not conclusive.	
1.2.9 If 1.2.8 is successful and time and funding are sufficient, report on probably time series of weather systems as suggested by the isotopic ratios in cave	31/12/2011	Complete, as modified.	The results were not as conclusive as originally hypothesised. This Milestone

structures to place the current rainfall changes in context			has been augmented with a literature review.